Nonuniformity in Natural Rubber As Revealed by Small-Angle Neutron Scattering, Small-Angle X-ray Scattering, and Atomic Force Microscopy

Takeshi Karino,[†,||] Yuko Ikeda,[*,‡] Yoritaka Yasuda,[‡] Shinzo Kohjiya,[§,⊥] and Mitsuhiro Shibayama[*,†,||]

Institute for Solid State Physics, The University of Tokyo, Kashiwa, Chiba 277-8581, Japan, Graduate School of Science and Technology, Kyoto Institute of Technology, Matsugasaki, Kyoto 606-8585, Japan, Institute for Chemical Research, Kyoto University, Uji, Kyoto 611-0011, Japan, and CREST, Japan Science and Technology Agency, 4-1-8 Honcho Kawaguchi, Saitama 332-0012, Japan

Received October 11, 2006; Revised Manuscript Received December 2, 2006

The microscopic structures of natural rubber (NR) and deproteinized NR (DPNR) were investigated by means of small-angle neutron scattering (SANS), small-angle X-ray scattering (SAXS), and atomic force microscopy (AFM). They were compared to those of isoprene rubber (IR), which is a synthetic analogue of NR in terms of chemical structure without any non-rubber components like proteins. Comparisons of the structure and mechanical properties of NR, DPNR, and IR lead to the following conclusions. (i) The well-known facts, for example, the outstanding green strength of NR and strain-induced crystallization, are due not much to the presence of proteins but to other components such as the presence of phospholipids and/or the higher stereoregularity of NR. It also became clear the naturally residing proteins accelerate the upturn of stress at low strain. The protein phases work as cross-linking sites and reinforcing fillers in the rubbery matrix. (ii) The microscopic structures of NR were successfully reproduced by SANS intensity functions consisting of squared-Lorentz and Lorentz functions, indicating the presence of inhomogeneities in bulk and thermal concentration fluctuations in swollen state, respectively. On the other hand, IR rubbers were homogeneous in bulk. (iii) The inhomogeneities in NR are assigned to protein aggregates of the order of 200 Å or larger. Although these aggregates are larger in size as well as in volume fraction than those of cross-link inhomogeneities introduced by cross-linking, they are removed by deproteinization. (iv) Swelling of both NR and IR networks introduces gel-like concentration fluctuations whose mesh size is of the order of 20 Å.

1. Introduction

Natural rubber (NR) is a unique biomass. It is only one polymeric hydrocarbon among many biopolymers whose source is almost always *Hevea brasiliensis*. It is one of the most important industrial materials among many polymeric ones. For example, NR is indispensable for pneumatic tires, especially the tires for heavy-duty uses, for example, tires for aircrafts and heavy trucks, and for rubber bearings in a seismic isolation system.[1,2] Also, thin NR films manufactured from NR latex, for example, surgical gloves, condoms, and rubber tubes in biomedical and health care fields, are very important materials. This versatility of NR in both industrial and hygienic applications is ascribable to its toughness based on its outstanding tensile properties and excellent crack growth resistance, which are assumed to be due to its ability to crystallize upon stretching.[1−13]

On the other hand, it is well known that NR contains non-rubber components such as proteins, phospholipids and fatty acids, carbohydrates, and inorganic substances.[14,15] Until recently, these non-rubber components of NR have been believed to be a factor to improve the mechanical properties of NR, and some of these were examined in how they interact with NR main chain.[2,16−20] However, no reports on the direct morphological evidence of non-rubber components in solid have been published as far as we know.

The presence of long-range inhomogeneities in rubbers, called cross-linking inhomogeneities (or heterogeneities), has been recognized as an important part in determining the mechanical properties of rubbers.[21−24] These inhomogeneities are inevitably introduced by cross-linking. Small-angle neutron scattering (SANS) has been one of the major tools to investigate the structure of polymeric systems since its first application to polymer science in 1973.[25,26] Both hydrogen/deuterium (H/D) labeling and H/D contrast matching techniques allow one to determine the size, orientation, and conformation of targeting polymer chains.[27] Hence, the inhomogeneities in rubbers can be amplified and visualized by swelling the rubber with a deuterated solvent as are the cases of polymer gels.[28]

In this study, SANS was used for the first time for morphological study of uncross-linked NR. Small-angle X-ray scattering (SAXS) and atomic force microscopy (AFM) were also performed to support the SANS results. To discuss the relationship between the structure and mechanical properties of uncross-linked NR, tensile testing was carried out. Although both latex and solid NR are generally utilized in the industry as commercial NR, the consumption of solid NR is much larger.

* Corresponding authors. E-mail: shibayama@issp.u-tokyo.ac.jp (M.S.); yuko@kit.jp (Y.I.).
† The University of Tokyo.
‡ Kyoto Institute of Technology.
§ Kyoto University.
|| CREST.
⊥ Present address: Visiting Professor, Faculty of Science, Mahidol University at Salaya, Puthamonton, Nakorn Phatom 73170, Thailand.

10.1021/bm060983d CCC: $37.00
Published on Web 01/23/2007

Table 1. Results of Elemental Analysis

	rubber samples		
	NR	DPNR	IR
carbon (wt %)	85.82	87.39	87.75
hydrogen (wt %)	11.80	11.88	12.04
nitrogen (wt %)	0.56	0.00	0.00

Thus, solid NR including deproteinized NR (DPNR) was employed in this work as well as isoprene rubber (IR), that is, a synthetic analogue of NR. Cross-linked NR and IR were also used for SANS experiments to elucidate cross-link inhomogeneities and local network structure.

2. Experimental Section

2.1. Rubber Samples. Raw rubber, that is, NR (RSS No. 1 from Indonesia), DPNR (DPNR 6110, Sumitomo Rubber Co.), and IR (IR 2200, JSR Co.), were used as received. The results of elemental analysis for these uncross-linked rubbers are shown in Table 1, which was performed at the Center for Organic Elemental Microanalysis, Kyoto University. Because of the difficulty of quantitative analysis for P, S, and other elements in NR, only the contents of C, H, and N in NR are shown in Table 1. Because NR is of very high molar mass, it was subjected to a two-roll milling (for ca. 5 min at room temperature) to obtain lower viscosity NR (NR0).

2.2. Cross-Linked Rubber Samples. Peroxide-cross-linked NR and IR samples were prepared as follows: NR or IR was mixed with dicumyl peroxide (DCP) on a two-roll mill. The mix was cured under a heat-pressing at 155 °C for 30 min in a mold to give a cross-linked rubber sheet of 1 mm thickness. The recipes of NR and IR mixes are shown in Table 2 together with network-chain density, ν, and degree of swelling of the cross-linked samples, Q.

2.3. Tensile Measurement. Tensile measurement was carried out at room temperature (ca. 25 °C) using a custom-made tensile tester (ISUT-2201, Aiesu Giken Co., Kyoto). Ring-shaped rubber samples were subjected to the tensile measurement. The inner and outer diameters of the samples were 11.7 and 13.7 mm, respectively. The stretching speed was 100 mm/min. The elongation ratio, α, is defined as $\alpha = l/l_0$, where l_0 and l are the sample lengths before and after deformation, respectively. From the results of tensile properties, the network-chain density ν was estimated on the basis of the classical theory of rubber elasticity using the equation $\sigma = \nu kT(\alpha - 1/\alpha^2)$, where σ is the stress, k is the Boltzmann constant, and T is absolute temperature.[29]

2.4. Swelling Measurement. The degree of swelling in volume, Q, of the peroxide-cross-linked rubber was measured. The sample specimens were swollen in toluene at 25 °C for 3 h, and their volume change was measured using CCD camera (VC1000 Digital Fine Scope, OMRON Co.). The degree of swelling was calculated using the equation $Q = V_s/V_0$, where V_0 and V_s are the volumes before and after swelling, respectively.

2.5. Atomic Force Microscopy. Atomic force microscopy (AFM) observation was conducted using a SPM-9600 scanning probe microscope (SHIMADZU Co.) at room temperature. The cantilevers used were NCHR (NANOWARLD) whose spring constant and resonance frequency were 40 N/m and 300 kHz, respectively. Phase mode was utilized for the observation. Force curve data were recorded for 256 × 256 points at a two-dimensional surface. The surface of each sample was prepared by breaking the frozen specimen after cooling in liquid-nitrogen.

2.6. Small-Angle X-ray Scattering (SAXS) Measurement. SAXS measurement for dry NR film was carried out at BL40B2 beam line in SPring-8 at room temperature. The wavelength of X-ray was 1.5 Å, and the camera length was ca. 3 m. The sample thickness was ca. 1.5 mm. The exposure time was 10 s. A 300 × 300 mm^2 square imaging plate with the resolution of 0.1 mm/pixel (Rigaku R-axis IV^{++}) was used for obtaining two-dimensional SAXS patterns and then circularly averaged. The observed scattering intensity was corrected for empty beam and transmission.

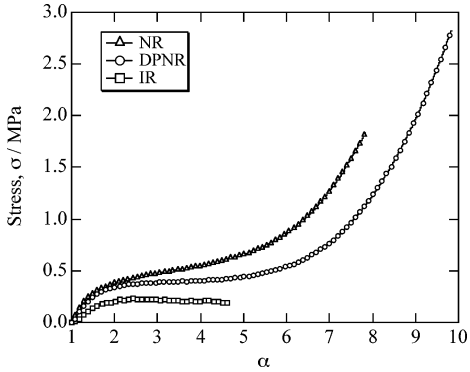

Figure 1. Stress-elongation ratio curves of NR, DPNR, and IR at room temperature.

2.7. Small-Angle Neutron Scattering (SANS) Measurement. Small-angle neutron scattering (SANS) experiments were carried out at SANS-U, Institute for Solid State Physics, The University of Tokyo. The wavelength was 7.00 Å. The sample-to-detector distances were chosen to be 2.00 and 8.00 m. The scattered intensity was collected with an area detector and then circularly averaged. The details of the instrument and data reduction are given elsewhere.[30,31] Dry and swollen samples with deuterium-toluene were subjected to SANS.

3. Results and Discussion

3.1. Mechanical Properties. Figure 1 shows stress-elongation ratio curves of the so-called "green" NR, DPNR, and IR films at room temperature, that is, uncross-linked NR, DPNR, and IR films. The ultimate tensile stresses ("green strength") of NR and DPNR are much higher than that of IR. Note that the "green strength" is an important mechanical property during the processing of tires. For both NR and DPNR films, the stress increased up to the break, ascribable to the strain-induced crystallization (SIC), via a flat region at the intermediate α's. On the other hand, IR has a very low elongation and strength at break. The stress of IR increased initially and leveled off above $\alpha \approx 2$. Because IR does not possess any non-rubber components originated from the plant, *Hevea brasiliensis*, and the stereoregularity of the *cis*-1,4-configuration is not as perfect as NR, the green strength is poor. When the tensile properties of uncross-linked NR film are compared to those of uncross-linked DPNR, it is noted that an increase of stress occurred at smaller α's in NR than DPNR. Generally, the increase of network-chain density in the rubber networks accelerates the upturn of stress due to SIC in the stress-elongation curves. Therefore, the difference in the stress-elongation behaviors between the NR and DPNR films shown in Figure 1 can be ascribed to the presence of proteins in the NR matrix, where the protein phases work as both cross-linking sites and fillers. Because the upturn of the stress of NR is due to the SIC behavior of polyisoprene segments, the observed results in this study were in good agreement with those of our recent studies on the SIC of sulfur-cross-linked NR and peroxide-cross-linked NR during in situ deformation: The sulfur-cross-linked NR crystallized much faster than IR during the post-stretch relaxation in the range of 8 s,[32] and peroxide-cross-linked NR progressed at lower strain with the increase of network-chain density.[33] Although differences in the mechanical properties between NR and IR are well known, the superiority of NR to IR has been little understood from microscopic points of view.

Table 2. Recipe and Properties of the Cross-Linked Rubber Samples

	sample code							
	NR02	NR06	NR10	NR30	IR02	IR06	IR10	IR30
rubber	100	100	100	100	100	100	100	100
DCP[a] (phr[b])	0.2	0.6	1.0	3.0	0.2	0.6	1.0	3.0
$\nu^c \times 10^4$ (mol/cm^3)	0.40	0.85	0.94	2.04	0.33	0.80	1.07	2.12
Q	12.7	6.5	6.4	4.0	10.7	5.6	5.9	3.8

[a] Dicumyl peroxide. [b] Part per one hundred rubber by weight. [c] Determined on the basis of classical theory of rubber elasticity.

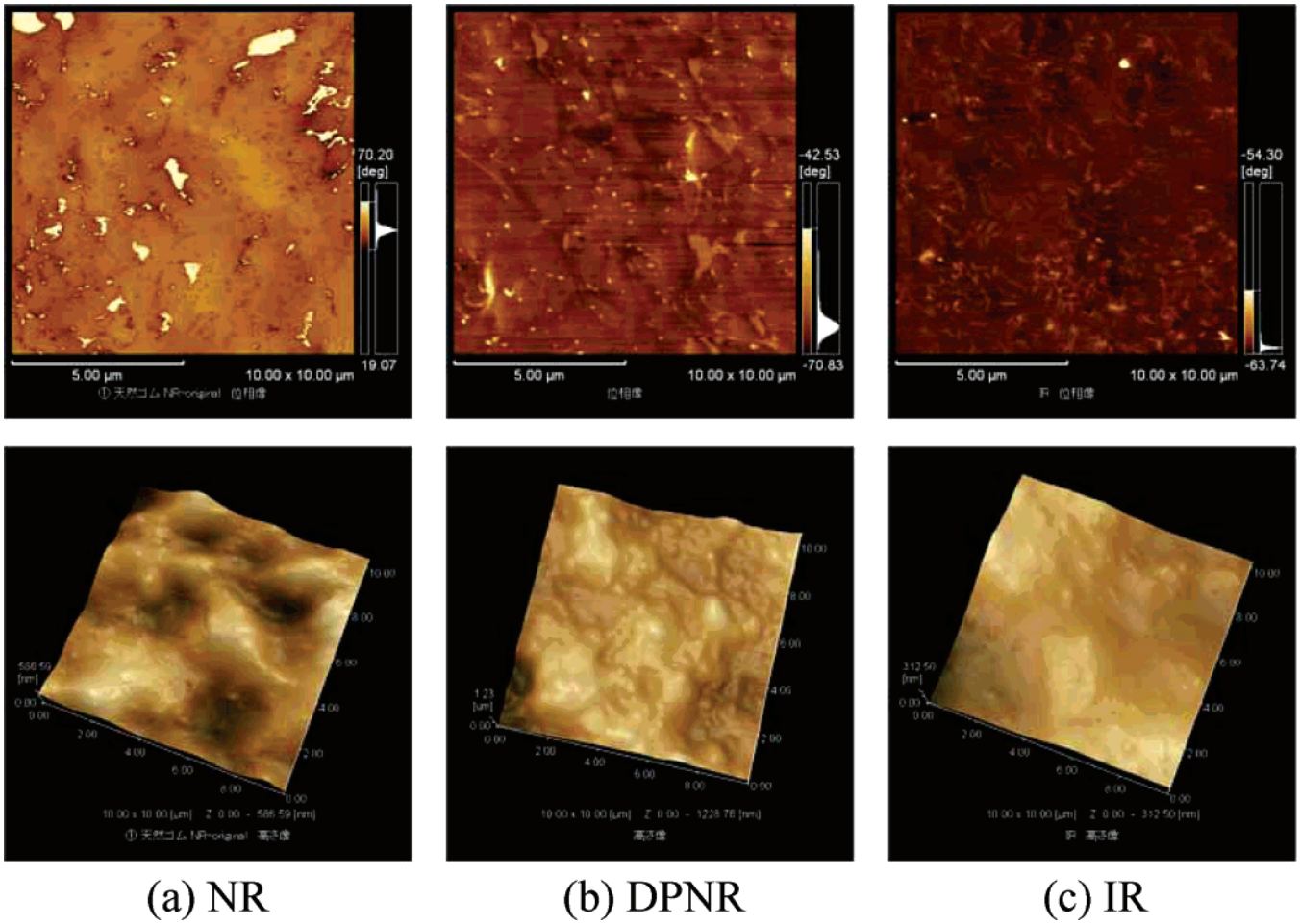

Figure 2. AFM photographs of samples cut after cooling in liquid nitrogen. (a) NR, (b) DPNR, and (c) IR. Upper, phase images; lower, topology images. The bright regions are harder than the dark regions (upper).

3.2. AFM. The presence of non-rubber components in NR and their morphology was confirmed by AFM observation. Figure 2 shows the AFM photographs of NR, DPNR, and IR. The upper and lower photographs are phase images and topology images, respectively. In their phase images, bright and dark parts mean hard and soft phases, respectively. It is noted that bright colored parts, that is, hard parts, were observed in the matrix of NR, whereas very small and moderate colored parts were detected in the matrixes of DPNR and IR. Because proteins were almost excluded in DPNR and they were not present at all in IR, the bright colored parts in NR are concluded to be protein phases. Their sizes were irregular. It is noted that this AFM observation is the first experimental result on the morphology of NR as far as we know.

3.3. SANS. *3.3.1. Bulk Polymer.* Figure 3 shows SAXS and SANS intensity functions, $I_{SAXS}(q)$ and $I_{SANS}(q)$, for NR and deproteinized NR (DPNR), where q is the magnitude of scattering vector. NR0 indicates natural rubbers after milling without addition of cross-linker. Here, the process of "milling" is expected to result in the lower viscosity of NR by chain scission. This figure implies several important facts. First, both SAXS (thin lines) and SANS intensity functions (symbols) are

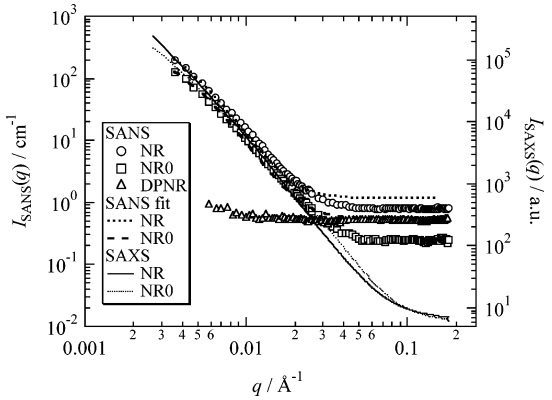

Figure 3. SANS (symbols) and SAXS curves (thin lines) of NR rubbers (a) before (NR) and (b) after milling (NR0) without cross-linker. The thick dotted and dashed lines denote the fit with eq 1.

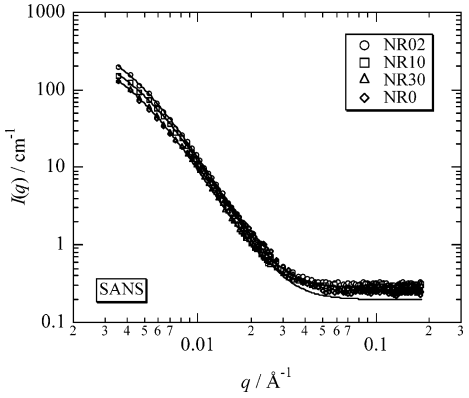

Figure 4. SANS curves of noncross-linked (NR0) and cross-linked NRs (NR02, NR10, NR30). The solid lines denote the fit with eq 1.

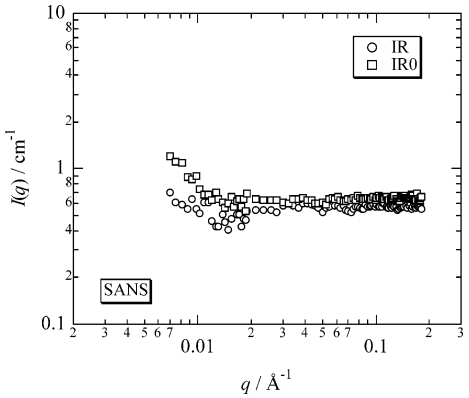

Figure 5. SANS curves of IR rubbers (a) before (IR) and (b) after milling (IR0) without cross-linker.

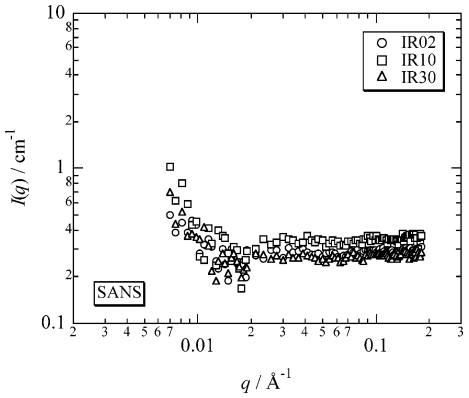

Figure 6. SANS curves of cross-linked IRs (IR02, IR10, IR30).

very similar and have a strong upturn at low q's. Note that it is not common that both SAXS and SANS show similar scattering functions. In particular, no characteristic scattering was expected in this study because NR had not been deuterium (D) labeled. Even so, the experimental results showed similar scattering functions. This indicates the presence of unknown compounds consisting of elements having similar scattering length, b_i, to D ($b_D = 6.671 \times 10^{-13}$ cm), such as N ($b_N = 9.36 \times 10^{-13}$ cm) and O ($b_O = 5.803 \times 10^{-13}$ cm) rather than that of H ($b_H = -3.741 \times 10^{-13}$ cm), and they play a role similar to that of D. As a result, similar scattering functions were observed in both cases. This clearly indicates that the same structure is observed by SAXS as well as by SANS. Second, deproteinization results in the disappearance of the upturn in $I_{SANS}(q)$ at low q's. Hence, it is concluded that the upturns in $I_{SAXS}(q)$ and $I_{SANS}(q)$ are assigned to be proteins inherently residing in natural rubbers. The flattening of $I_{SANS}(q)$ at $q \geq 0.03$ Å^{-1} is due to incoherent

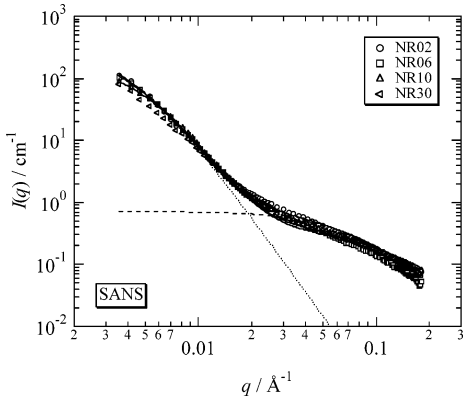

Figure 7. SANS intensity functions of cross-linked NRs. The dotted and dashed lines are the fit with SL- and L-functions for NR02, respectively.

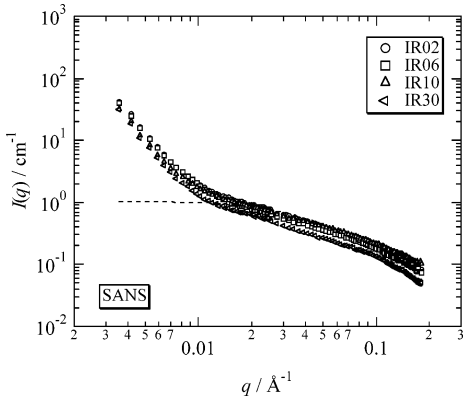

Figure 8. SANS intensity functions of cross-linked IRs. The dashed line is the fit with L-functions for IR02.

scattering from proteins, which are not perfectly subtracted in background subtraction procedure. The thick dotted and dashed lines show the result of curve fits, respectively, for NR and NR0, with a squared-Lorentz function (SL-function) given by

$$I(q) = I_{SL}(0)/(1 + \Xi^2 q^2)^2 \quad (1)$$

where Ξ is the characteristic size of inhomogeneities. The SL-function is often used to represent cross-link (or structure) inhomogeneities in gels[28,34] as well as to describe two-phase systems having random orientation with its chord length of Ξ.[35] Note that an offset baseline, representing incoherent scattering originating mainly hydrogen atoms in protein, is added to eq 1 to represent the q-independent scattering at large q's ($q \geq 0.03$ Å^{-1}). As shown in the figure, the curve fitting is quite successful and the values of Ξ were evaluated to be 256 and 237 Å, respectively, for NR and NR0. Hence, noncross-linked NRs have a well-developed two-phase structure consisting of polyisoprene matrix and non-rubber components.

Figure 4 shows SANS intensity functions of noncross-linked NR (NR0) and cross-linked NRs (NR02, NR10, and NR30). Although $I_{SANS}(q)$ slightly decreases with increasing cross-link concentration, the change seems to be negligible. It is interesting to note that the protein aggregates in the rubbery matrix seemed to be maintained even after the curing (at 155 °C for 30 min). The solid lines are curve fits with eq 1, which again support the validity of the applicability of eq 1. The values of Ξ are very similar to the case of noncross-linked rubbers as will be discussed later.

Figures 5 and 6 show the SANS intensity functions for synthetic poly(isoprene), IR, before (Figure 5) and after cross-

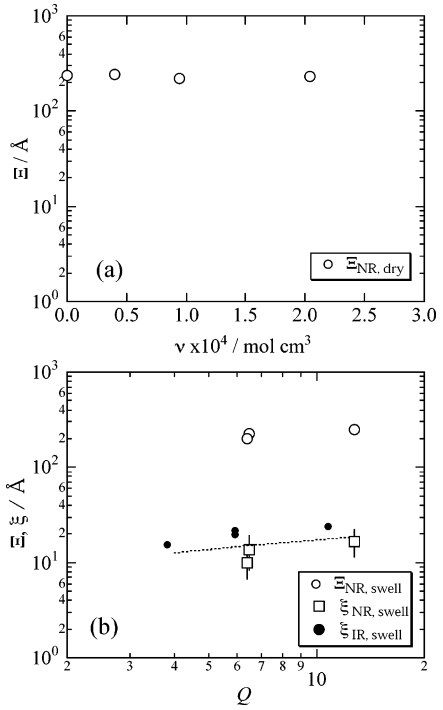

Figure 9. (a) Network-chain density dependence, ν, of Ξ. (b) The degree of swelling, Q, dependence of Ξ and ξ.

linking (Figure 6). For noncross-linked IR (IR and IR0), $I_{SANS}(q)$ is rather q-independent except for the region below $q = 0.01$ Å^{-1}. Although an upturn is observed for $q \leq 0.01$ Å^{-1}, it may be due to inhomogeneities inherent of IR. However, it is much smaller than that observed in NRs. Note that no significant cross-link concentration dependence is observed (Figure 6). The effect of aggregates of proteins on the mechanical properties of cross-linked NR will be reported after discriminating it from the effect of cross-linking.

3.3.2. Swollen Networks. Figure 7 shows SANS intensity functions for swollen NRs having different network-chain densities. The dotted and dashed lines denote the result of curve fit for NR02 with a squared-Lorentz (SL) function (dotted line) and with a Lorentz (L) function (dashed line).[36] Here, the L-functions are given by

$$I(q) = I_L(0)/(1 + \xi^2 q^2) \qquad (2)$$

where ξ is the correlation length. On the other hand, the L-function is commonly used to describe polymers in semidilute solutions.[37] As shown in the figure, the observed scattering function is well fitted with the calculated scattering function with $\xi = 16.4$ Å. Note that this value does not correspond to the inter-cross-link distance, but a mesh size consisting of entangled network.[28]

A similar analysis was carried out for IRs (IR02, IR06, IR10, and IR30), and the result is shown in Figure 8. The dashed line denotes the fit for IR02. This figure also shows that the scattering functions are well represented by Lorentz functions given by eq 2. Very little network-chain density dependence was observed in $I(q)$. This may be due to the fact that the polymer concentration is too high to discriminate network-chain density dependence. The upturn in $I(q)$ at low q's originates from cross-link inhomogeneities amplified by swelling with a deuterated solvent.[28]

Figure 9 shows (a) the network-chain density, ν, dependence of the characteristic length of inhomogeneities, Ξ, and (b) the degree of swelling, Q, dependence of ξ and Ξ for NR and IR.

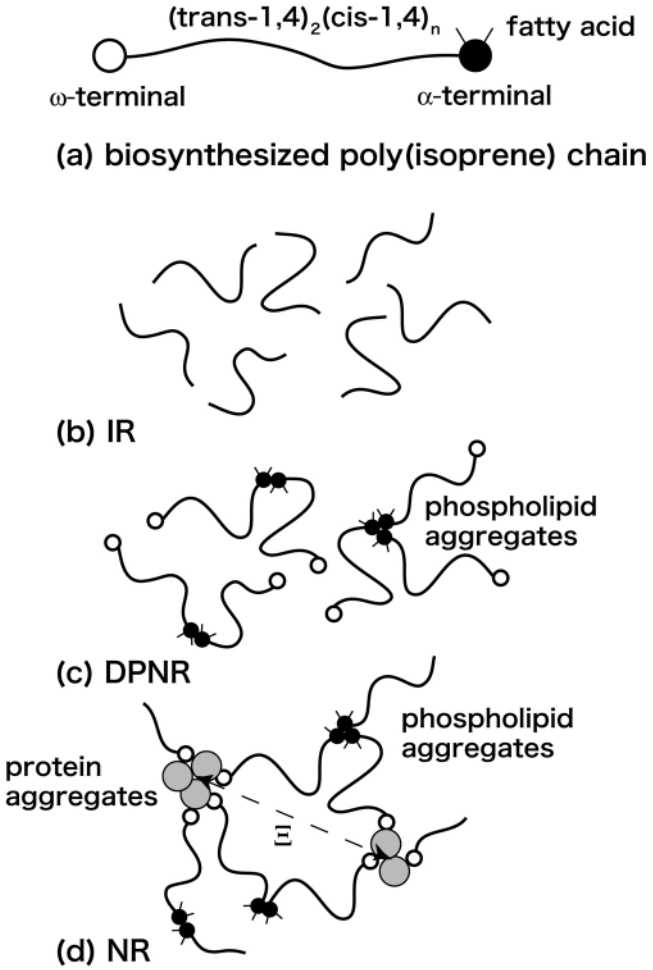

Figure 10. Schematic illustration of the microstructures of (a) biosynthesized polyisoprene, (b) IR, (c) DPNR, and (d) NR. The strong green strength in NR and DPNR is due to cross-linked structure of polyisoprene via phospholipids. NR contains protein aggregates that play as filler and additional cross-linkers.

It is noted that Ξ of NR does not vary with changing network-chain density. This indicates that inhomogeneities inherent of NR are very large due to the presence of non-rubber components and network-chain density dependence is insignificant. On the other hand, ξ and Ξ can be scaled with $\xi \approx Q^{1/3}$ and $\Xi \approx Q^{1/3}$, suggesting that both protein domains and mesh size are deformed affinely by swelling.

3.4. Structure of NR. It is well known that NR is standing alone among the general-purpose rubbers; especially tread rubbers for pneumatic tires used under heavy conditions for aircrafts and heavy-duty trucks are usually made from NR. Until recently, the non-rubber components of NR such as proteins have been suggested to be a factor to improve the mechanical properties of NR,[2,16,17,19] particularly on filler-loaded NR. However, there is no direct morphological evidence to support this view. Tanaka presumed a network structure formed by aggregation of proteins and phospholipids in polyisoprene segments,[20] where α-terminal and ω-terminal groups of main chain of NR interact with phospholipids and proteins, respectively. Thus, the structure of NR has been believed to be a physical gel (the network by physical interactions). Our experimental findings support this model of NR. Figure 10 schematically represents the structure of (a) biosynthesized poly(isoprene), (b) IR, (c) DPNR, and (d) NR. Here, cartoons are drawn on the basis of the model proposed by Tanaka,[20,38] while the new findings on the aggregation of non-rubber components

exclusively observed in NR, for example, the distance between protein aggregates, are incorporated. IR consists of polyisoprene chains without any functional groups (Figure 10b). DPNR consists of cross-linked polyisoprene chains with phospholipid domains via α-terminal groups (Figure 10c). NR has a more sophisticated structure. Protein aggregates, spaced by the distance of Ξ, combine NR chains and play as a filler or an additional cross-linker as depicted in Figure 10d. These aggregates disappear by deproteinization. Because both NR and IR comprise essentially with polyisoprene chains, both of them have a similar chemical network structure with a mesh size of ξ in the swollen state.

4. Conclusion

The microscopic structures of natural rubbers (NR) were investigated by means of AFM, SAXS, and SANS and were compared to those of isoprene rubber (IR). The following facts were disclosed. (1) The SANS intensity function of noncross-linked NR is given by a squared-Lorentz function (SL), $I(q) = I_{SL}(0)/(1 + \Xi^2 q^2)^2$, while those of deproteinized NR (DPNR) and IR show no q-dependence, where q is the magnitude of scattering vector and Ξ is the characteristic length of inhomogeneities. (2) Although cross-linking of NR does not lead to any change in intensity, that of IR results in an increase in scattering intensity represented by SL functions, indicating the appearance of cross-link inhomogeneities. (3) Swelling of NR and IR rubbers leads to an appearance of Lorentz (L) function, $I(q) = I_L(0)/(1 + \xi^2 q^2)$, representing a gel-type swollen network structure with a mesh size of ξ. Hence, it is given by a combination of SL- and L-functions. (4) These results are well correlated with AFM observation. Comparisons of the structure and mechanical properties of NR, DPNR, and IR lead to the following conclusions. (i) The well-known facts, for example, the outstanding green strength of NR and strain-induced crystallization, are due not much to the presence of proteins but to other components such as the presence of phospholipids and/or the higher stereoregularity of NR. The presence of other constituents such as phospholipids and/or the higher stereoregularity of NR is the most probable candidate to be responsible for the unique properties of NR. However, it also became clear that the proteins accelerate the upturn of stress at low strain, which is ascribable to the aggregation of proteins. The protein phases work as cross-linking sites and reinforcing fillers in the rubbery matrix. (ii) The inherent inhomogeneities of NR are much larger in size (≥200 Å) as well as in volume fraction than those of cross-link inhomogeneities introduced by cross-linking. These inhomogeneities are removed by deproteinization. (iii) Swelling of rubbers introduces gel-like concentration fluctuations whose mesh size is of the order of 20 Å.

Acknowledgment. This work is supported by Core Research for Evolutional Science and Technology (CREST), Japan Science and Technology Agency, Japan. T.K. acknowledges the support by CREST. This work was partially supported by the Ministry of Education, Science, Sports, and Culture, Japan (Grant-in-Aid 18205025). The SANS experiment was performed with the approval of the Institute for Solid State Physics, The University of Tokyo (Proposal No. 6539), at the Japan Atomic Energy Research Institute Agency, Tokai, Japan. The synchrotron radiation experiment on SAXS was performed at the BL-40B2 in the SPring-8 with the approval of the Japan Synchrotron Radiation Research Institute (JASRI) (Proposal No. 2006A1298-NL2b-np). This work was supported by Research Grants from the President of KIT 2006. We thank Shimadzu Co. for its assistance with AFM observations.

References and Notes

(1) Bateman, L. *The Chemistry and Physics of Rubber-like Substances*; MacLaren & Sons: London, 1963.
(2) Roberts, A. D. *Natural Rubber Science and Technology*; Oxford University Press: Oxford, 1988.
(3) Mitchell, G. R. A wide-angle X-ray study of the development of molecular orientation in crosslinked natural rubber. *Polymer* **1984**, *25*, 1562−1572.
(4) Mandelkern, L. The role of elastomers in the study of polymer crystallization. *Rubber Chem. Technol.* **1993**, *66*, G61−G75.
(5) Murakami, S.; Senoo, K.; Toki, S.; Kohjiya, S. Structural development of natural rubber during uniaxial stretching in situ wide angle X-ray diffraction using a synchrotron radiation. *Polymer* **2002**, *43*, 2117−2120.
(6) Toki, S.; Sics, I.; Ran, S.; Liu, L.; Hsiao, B. S.; Murakami, S.; Senoo, K.; Kohjiya, S. New insights into structural development in natural rubber during uniaxial deformation by in situ synchrotron X-ray diffraction. *Macromolecules* **2002**, *35*, 6578−6584.
(7) Trabelsi, S.; Albouy, P.-A.; Rault, J. Stress-induced crystallization around a crack tip in natural rubber. *Macromolecules* **2002**, *35*, 10054−10061.
(8) Miyamoto, Y.; Yamao, H.; Sekimoto, K. Crystallization and melting of polyisoprene rubber under uniaxial deformation. *Macromolecules* **2003**, *36*, 6462−6471.
(9) Tosaka, M.; Murakami, S.; Poompradub, S.; Ikeda, Y.; Kohjiya, S.; Toki, S.; Sics, I.; Hsiao, B. S. Orientation and crystallization of natural rubber network as revealed by WAXD using synchrotron radiation. *Macromolecules* **2004**, 3299−3309.
(10) Tosaka, M.; Kohjiya, S.; Murakami, S.; Poompradub, S.; Ikeda, Y.; Toki, S.; Sics, I.; Hsiao, B. S. Effect of network-chain length on strain-induced crystallization of NR and IR vulcanizates. *Rubber Chem. Technol.* **2004**, *77*, 711−723.
(11) Le Cam, J.-B.; Huneau, B.; Verron, E.; Gornrt, L. Mechanism of fatigue crack growth in carbon black filled natural rubber. *Macromolecules* **2004**, *37*, 5011−5017.
(12) Poompradub, S.; Tosaka, M.; Kohjiya, S.; Ikeda, Y.; Toki, S.; Sics, I.; Hsiao, B. S. Mechanism of strain-induced crystallization in filled and unfilled natural rubber vulcanizates. *J. Appl. Phys.* **2005**, *97*, 103529/1−103529/9.
(13) Kohjiya, S.; Tosaka, M.; Furutani, M.; Ikeda, Y.; Toki, S.; Hsiao, B. S. Role of stearic acid in the strain-induced crystallization of crosslinked natural rubber and synthetic *cis*-1,4-polyisoprene. *Macromolecules*, submitted.
(14) Archer, B. L.; Barnard, D.; Cockbain, E. G.; Dickenson, P. B.; McMullen, A. I. Chapter 3, Structure, Composition and Biochemistry of Hevea Latex. In *The Chemistry and Physics of Rubber-like Substances*; Bateman, L., Ed.; MacLaren & Sons: London, 1963.
(15) Wititsuwannakul, D.; Wititsuwannakul, R. Chapter 6, Biochemistry of Natural Rubber and Structure of Latex. In *Biopolymers Vol. 2: Polyisoprenoids*; Koyama, T., Steinbuchel, A., Eds.; Wiley-VCH: Weinheim, 2001.
(16) Gregg, C. E.; Macey, J. H. Relation of properties and synthetic polyisoprene and natural rubber in the factory. Effect of non-rubber constituents of natural rubber. *Rubber Chem. Technol.* **1973**, *46*, 47−66.
(17) Lu, F. J.; Hsu, S. L. A vibrational spectroscopic analysis of the structure of natural rubber. *Rubber Chem. Technol.* **1987**, *60*, 647−658.
(18) Shibashi, T.; Hirose, K.; Tagata, N. Gel structures of natural rubber and synthetic isoprene rubber. *Kobunshi Ronbunshu* **1989**, *46*, 465−472.
(19) Marinovic, T.; Kralj-Novak, M.; Veksli, Z. Relation between the matrix inhomogenity and mechanical properties of natural rubber. *Kautsch. Gummi Kunstst.* **1992**, *45*, 190−192.
(20) Tanaka, Y. Structural characterization of natural polyisoprene: solve the mystery of natural rubber based on structural study. *Rubber Chem. Technol.* **2001**, *74*, 355−375.
(21) Stein, R. S. The determination of the inhomogeneity of crosslinking of a rubber by light scattering. *J. Polym. Sci.* **1969**, *B7*, 657−660.
(22) Bueche, F. Light scattering from swollen gels. *J. Colloid Interface Sci.* **1970**, *33*, 61−66.
(23) Pines, E.; Prins, W. The effect of nonrandom crosslinking on the light scattering of swollen polymer networks. *J. Polym. Sci.* **1972**, *B10*, 719−724.

(24) Mark, J. E.; Erman, B. *Rubberlike Elasticity A Molecular Primer*; Wiley: New York, 1988.
(25) Benoit, H.; Decker, D.; Higgins, J. S.; Picot, C.; Cotton, J. P.; Farnoux, B.; Jannink, G.; Ober, R. Dimensions of flexible polymer chains in the bulk and in solutions. *Nat. Phys. Sci.* **1973**, *24*, 13−15.
(26) Sadler, D. M. Neutron Scattering from Solid Polymers. In *Comprehensive Polymer Science*; Booth, C., Price, C., Eds.; Pergamon Press: Oxford, UK, 1989; Vol. 2.
(27) Higgins, J. S.; Benoit, H. C. *Polymers and Neutron Scattering*; Clarendon Press: Oxford, 1994.
(28) Shibayama, M. Spatial inhomogeneity and dynamic fluctuations of polymer gels. *Macromol. Chem. Phys.* **1998**, *199*, 1−30.
(29) Treloar, L. R. G. *The Physics of Rubber Elasticity*; Clarendon Press: Oxford, 1975.
(30) Okabe, S.; Nagao, M.; Karino, T.; Watanabe, S.; Adachi, T.; Shimizu, H.; Shibayama, M. Upgrade of the 32 m small-angle neutron scattering instrument, SANS-U. *J. Appl. Crystallogr.* **2005**, *38*, 1035−1037.
(31) Okabe, S.; Karino, T.; Nagao, M.; Shibayama, M. Current status of the 32 m small-angle neutron scattering instrument, SANS-U. *Nucl. Instrum. Methods Phys. Res., Sect. A*, submitted.
(32) Tosaka, M.; Kawakami, D.; Senoo, K.; Kohjiya, S.; Ikeda, Y.; Toki, S.; Hsiao, B. S. Crystallization and stress relaxation highly stretched samples of natural rubber and its synthetic analogue. *Macromolecules* **2006**, *39*, 5100−5105.
(33) Ikeda, Y.; Yasuda, Y.; Makino, S.; Yamamoto, S.; Tosaka, M.; Senoo, K.; Kohjiya, S. Strain-induced crystallization of peroxide-crosslinked natural rubber. *Polymer*, submitted.
(34) Onuki, A. Scattering from deformed swollen gels with heterogeneities. *J. Phys. II France* **1992**, *2*, 45−61.
(35) Debye, P.; Bueche, A. M. Scattering by an inhomogeneous solid. *J. Appl. Phys.* **1949**, *20*, 518−525.
(36) Shibayama, M.; Isono, K.; Okabe, S.; Karino, T.; Nagao, M. SANS study on pressure-induced phase separation of poly(*N*-isopropylacylamide) aqueous solutions and gels. *Macromolecules* **2004**, *37*, 2909−2918.
(37) de Gennes, P. G. *Scaling Concepts in Polymer Physics*; Cornell University: Ithaca, NY, 1979.
(38) Tanaka, Y.; Kawahara, S.; Tangpakdee, J. Structural characterization of natural rubber. *Kautsch. Gummi Kunstst.* **1997**, *50*, 6−11.

BM060983D